

ATLAS Internal Note
INDET-NO-103
5 April 1995

Radiation Hard Microstrip Gallium Arsenide Detectors

Chmill V.B.* , Chuntonov A.V.* , Khludkov S.S.+ , Koretski A.A.+ ,
Potapov A.I.+ , Smith K.M.°, Smoll A.V.* , Tolbanov O.P.+ , Vorobiev A.P.*

*Institute of High Energy Physics, Protvino, Russia.

+Siberian Institute for Physics and Technology, Tomsk, Russia.

°University of Glasgow, Glasgow, UK.

Introduction.

Our previous studies [1] have shown that GaAs doped with *Cr* or *Fe* can be used for the fabrication of radiation hard [2] position-sensitive detectors, which meet the requirements of the ATLAS experiment [3] for the operating conditions at the LHC. In this paper we present results from the first prototypes of microstrip GaAs detectors of this type tested in high energy accelerator beams and with β - particles from a radioactive ^{106}Ru source. This work forms part of the RD8 detector R.&D. research programme [4].

1 The main parameters of GaAs detectors.

The first GaAs detector prototypes employed three types of intrinsic structure: $p\text{-}\pi\text{-}\nu\text{-}n$, $n^+\text{-}\pi\text{-}\nu\text{-}n$, and $(\text{Au})n^+\text{-}\pi\text{-}\nu\text{-}n$, developed at the Siberian Institute for Physics and Technology, (SITP), Tomsk. For these detectors, the GaAs industry-standard substrate Czochralski material. The detectors, with surface area $20 \times 30 \text{ mm}^2$, were made on $350\mu\text{m}$ thick wafers of low-resistivity n -type GaAs, in which a high resistivity $100 \pm 50 \mu\text{m}$ thick layer was formed by means of chromium diffusion. Inside this layer we have a $\pi\text{-}\nu$ junction at a depth of $50 \pm 20 \mu\text{m}$ (Fig. 1). The readout strips, with pitch $150 \mu\text{m}$ and strip width $50 \mu\text{m}$, were formed from p -type or n^+ -type or n^+ -type GaAs with Au on top, .

The $I\text{-}V$ characteristics for the $(\text{Au})n^+\text{-}\pi\text{-}\nu\text{-}n$ and $p\text{-}\pi\text{-}\nu\text{-}n$ detectors, measured for a single strip, are presented in Fig. 2 and Fig. 3. The $p\text{-}\pi\text{-}\nu\text{-}n$ detectors display a characteristic diode shape with the forward and reverse currents differing by a few orders of magnitude. The $(\text{Au})n^+\text{-}\pi\text{-}\nu\text{-}n$ detector does not show such behaviour, however, because we have here two back-to-back junctions, $n^+\text{-}\pi$ and $\pi\text{-}\nu$, and a correspondingly low forward current. Here "forward" and "reverse" bias refers to the $\pi\text{-}\nu$ junction.

For tests in charged particle beams, we selected the $(\text{Au})n^+\text{-}\pi\text{-}\nu\text{-}n$ detectors, in which we observe the largest signals with current sensitive amplifiers, because of the low resistivity of the readout strips. Two versions of the $(\text{Au})n^+\text{-}\pi\text{-}\nu\text{-}n$ microstrip detectors were produced, with pitch 150 and $50 \mu\text{m}$ and strip width 50 and $10 \mu\text{m}$ respectively. The $p\text{-}\pi\text{-}\nu\text{-}n$ detectors were very noisy and were not used in the beam tests.

2 Measurements with a source.

For the initial evaluation of the *GaAs* microstrip detectors we measured the response of the $(Au)n^+-\pi-\nu-n$ $150\ \mu m$ pitch detectors to a ^{106}Ru β source, using current sensitive "Garantiya" [5] amplifiers D.C. coupled to the strips for the first amplification stage, a *LeCROY* 2249A CAMAC ADC and appropriate trigger electronics. Pulse height spectra were taken in the self-triggering mode with a trigger gate width of $20\ ns$. Fig. 4. shows the spectrum due to $2\ MeV$ electrons (minimum ionizing particles) from a radioactive ^{106}Ru source in a single strip $n^+-\pi$ junction of the $150\ \mu m$ pitch detector. This agrees well with a Landau distribution for ionizing losses in a thin layer of matter. The most probable signal ($\sim 14 \cdot 10^3$ electrons) is not high because of the small thickness of the sensitive region. The behaviour of this signal as a function of bias voltage is presented in Fig. 5. The full depletion voltage for the detector is near $200\ V$.

The signals from a single strip $\pi-\nu$ junction are in ~ 5 times smaller and compatible with noise. By contrast, if we compare the signals of these two junctions with those of $2 \times 2\ mm^2$ pad detectors, made using the same material and the same process technology, we see nearly equal signals from the β -source (Fig. 6). We explain these facts as follows.

In the case of microstrip detectors the reverse bias voltage ($\pi-\nu$ junction is working) builds a space charge region (SRC), that grows with increasing bias voltage into the ν -region. The π -region, with a resistivity $\sim 10^9\ Ohm \cdot cm$ and thickness $20 - 50\ \mu m$, acts here as a resistive layer between the SCR and the n^+ strips, and as a result the signals on the readout strips are small.

3 The charged particle beam test results.

The detection efficiency of a $150\ \mu m$ pitch detector was first studied in a $40\ GeV/c\ \pi^-$ beam at IHEP. To generate a trigger from beam particles we used upstream beam counters S_1, S_2 , a scintillator fibre counter placed close to the microstrip detector, with the fibre diameter $300\ \mu m$ orientated along the *GaAs* detector strips, and a $0.7 \times 1\ cm^2$ finger counter perpendicular to the fibre.

Fig. 7. shows the spectrum of signals from a single strip at $300\ V$ bias voltage. The most probable signal corresponds to $12 \cdot 10^3$ electrons and the

signal-to-noise ratio is approximately 6. From the "shadow" of the fibre (Fig. 8.) on the detector the detection efficiency can be estimated to be no more than 50%.

Similar measurements made with a $50 \mu m$ pitch detector in the $70 \text{ GeV}/c$ proton beam at IHEP give the spectrum and the fibre "shadow" profile presented in Fig. 9 and Fig 10. The most probable signal is equal to $10 \cdot 10^3$ electrons and the signal-to-noise ratio is near to 7. These measurements were made in quite a noisy environment as can be seen from Fig. 9. Taking in to account events with charge division between adjacent strips and accidental events we estimate the detection efficiency of the $50 \mu m$ pitch detector to be 76% for signals greater than $4 \cdot \sigma_{noise}$ and 98% for signals greater than $3 \cdot \sigma_{noise}$.

In a $5 \text{ GeV}/c \pi^-$ beam at CERN the same detector shows a better signal-to-noise ratio ~ 9.6 at a bias voltage of 75 V (Fig. 11). The charge cluster probability for the $50 \mu m$ pitch detector was measured with the following definition of a cluster for each event. First of all strip signals were scanned to find those strips with a signal higher than threshold. If any such channel was found, all neighboring strips with a signal above $(1.5 - 3.5) \cdot \sigma_{noise}$ were included in the cluster. In Table 1. we present the charge cluster probability for $50 \mu m$ and $150 \mu m$ pitch detectors. As expected for detectors with a large readout pitch and without intermediate strips, for most particles crossing the detector perpendicularly the charge will be collected mainly by one strip.

4 Conclusions

The results presented above are the first from microstrip detectors fabricated using the technology developed at SPTI, and are already very encouraging. Improved performance is expected from the next generation of devices, in which the sensitive thickness has been made almost equal to the physical thickness of the wafer material and efforts have been made to reduce the leakage current density. Further work is in progress on verifying the radiation hardness of the detectors to neutron, pion and proton radiation to the levels predicted for the LHC. If the high radiation tolerance of earlier samples continues to be observed in the newer batch, it may reasonably be claimed that these devices represent the strongest candidates for precision semiconductor tracking in the highest radiation zones of the LHC experiments.

CLUSTER PROBABILITY						
Detectors type	1 strip	2 strips	3 strips	4 strips	5 strips	Threshold
pitch 50 μm pitch 150 μm	66 % 63 %	26 % 29 %	3.6 % 5.8 %	3 % 1.6 %	0.6 % 0.7 %	1.5 σ
pitch 50 μm pitch 150 μm	73 % 78 %	23 % 19.7 %	0.6 % 1.8 %	2.4 % 0.3 %	0.6 % 0.09 %	2 σ
pitch 50 μm pitch 150 μm	80 % 88 %	16 % 11.5 %	1.8 % 0.5%	1.8 % 0.07 %	0.4 % 0.01 %	3 σ
pitch 50 μm pitch 150 μm	84 % 92.7 %	14 % 7 %	0.6 % 0.17 %	1.4 % 0.05 %	0 % 0.02 %	3.5 σ

References

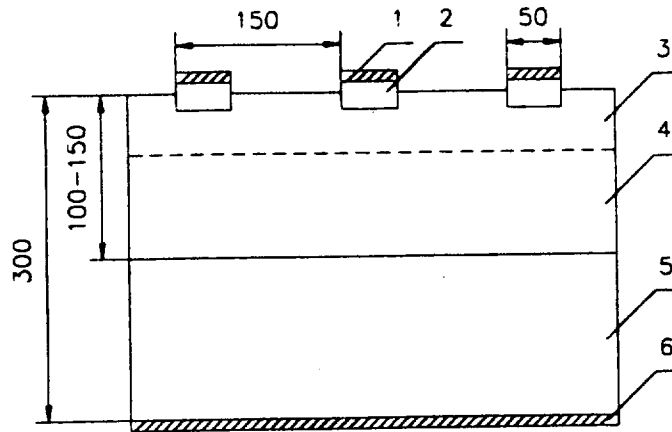
- [1] V.B. Chmill et al., Nucl. Instr. and Meth. A326(1993) 310
V.B. Chmill et al., Nucl. Instr. and Meth. A340(1994) 328

- [2] V.B. Chmill et al., ATLAS Internal Note, INDET-NO-036, 3rd February 1994. be published in "Journal of Physics D"

- [3] ATLAS Technical Proposal, CERN/LHCC/94-43, LHC/P2, 15 December 1994

- [4] The *GaAs* Collaboration, CERN/DRDC 94-32
RD8 Status Report, October 5, 1994

- [5] V.M. Golovin et. al., Preprint IHEP 89-231, Protvino, Russia (1989)



All sizes are in micrometers.

Figure 1: Intrinsic structure $(Au)n^+-\pi-\nu-n$ type.

1. Ohmic contact $Au - n^+$.
2. Microstrip n^+ - type.
3. π - layer.
4. ν - layer.
5. Substrate n - type.
6. Ohmic contact $Au - n$.

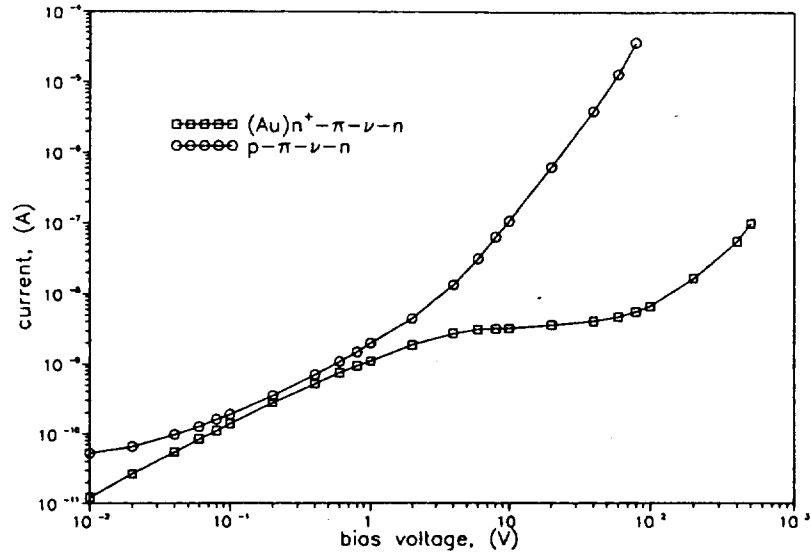


Figure 2: The forward branch of I - V characteristics.

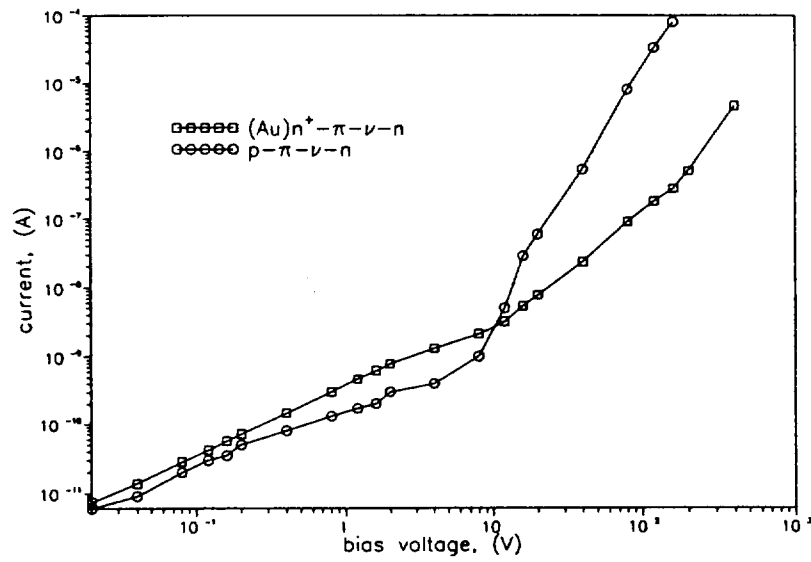


Figure 3: The reverse branch of I - V characteristics.

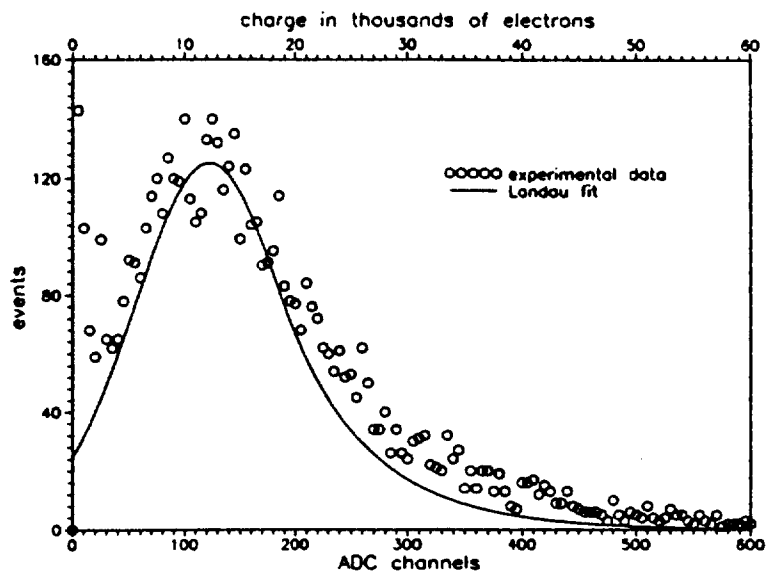


Figure 4: The spectrum of signals for single strip due to $E = 2 \text{ MeV}$ electrons.

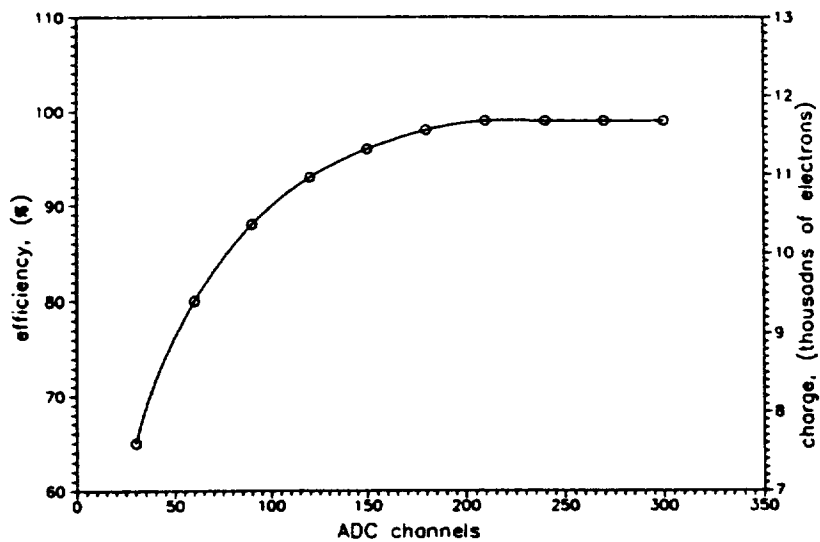


Figure 5: The behaviour of signal as a function of bias voltage.

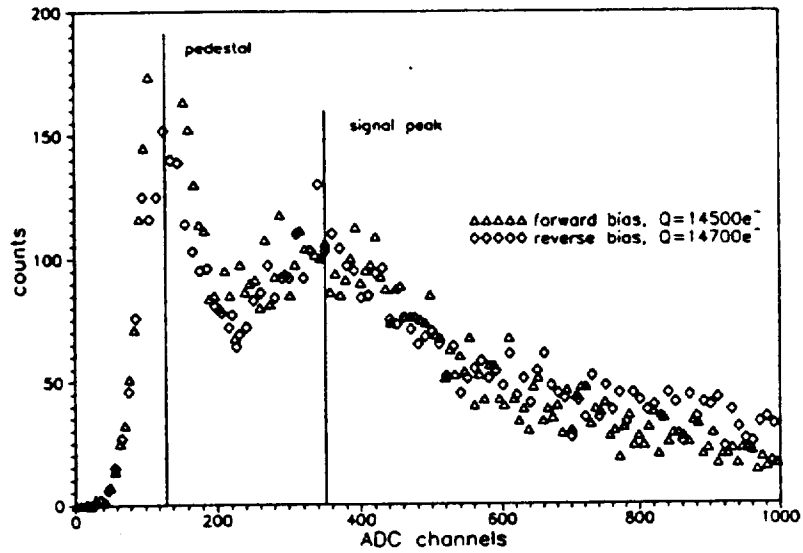


Figure 6: Spectra of the signals for a pad detector with different polarity of bias voltage.

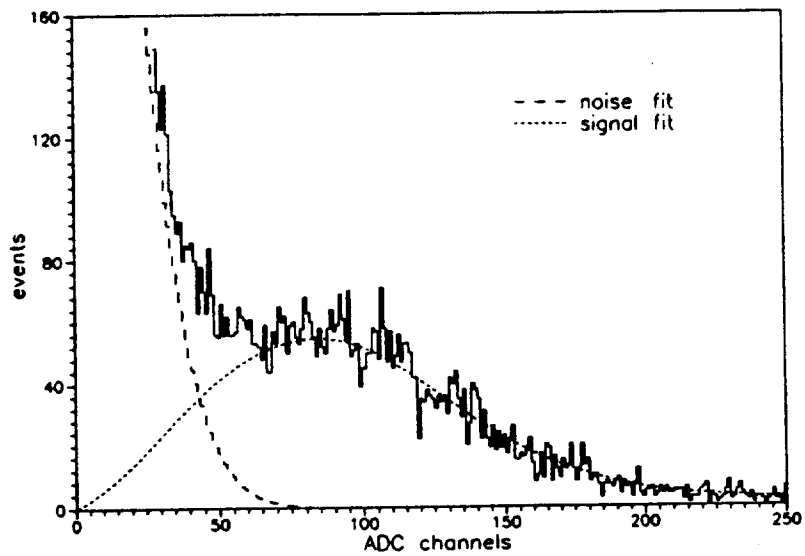


Figure 7: Spectrum of the signals for a single strip (pitch $150 \mu m$).

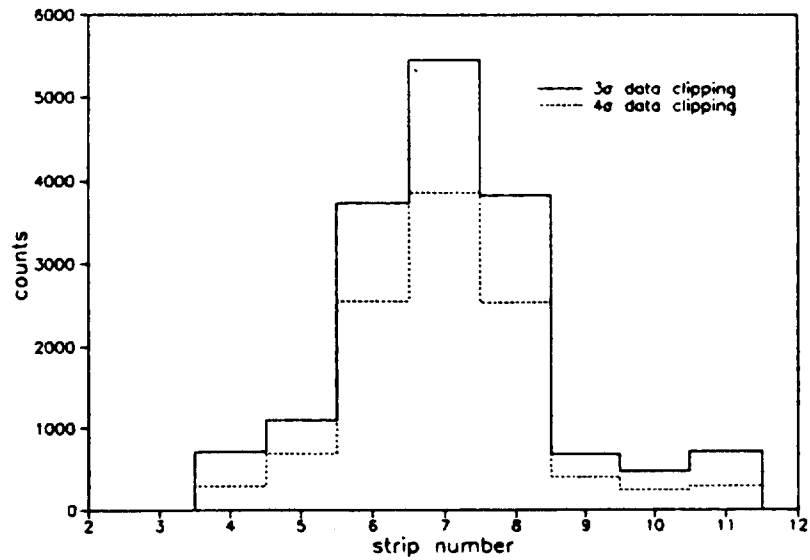


Figure 8: "Shadow" of the fibre (pitch $150 \mu m$).

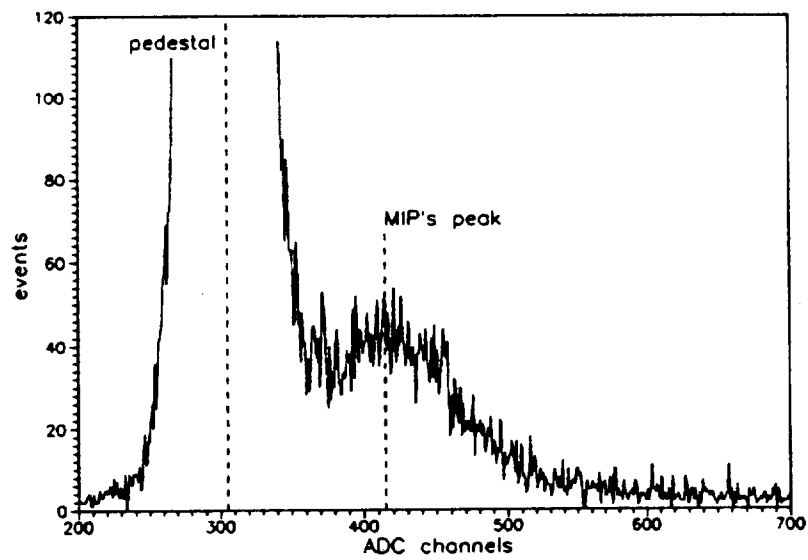


Figure 9: Spectrum of the signals for a single strip (pitch $50 \mu m$).

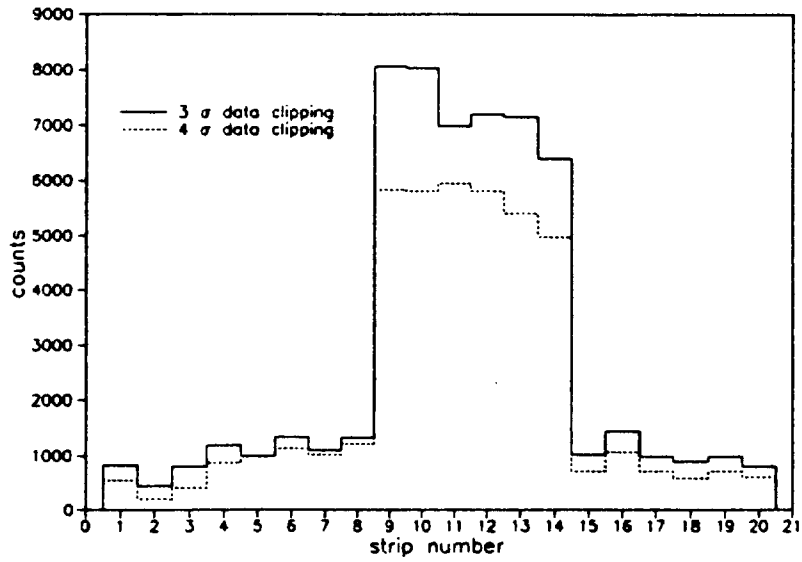


Figure 10: "Shadow" of the fibre (pitch $50 \mu m$).

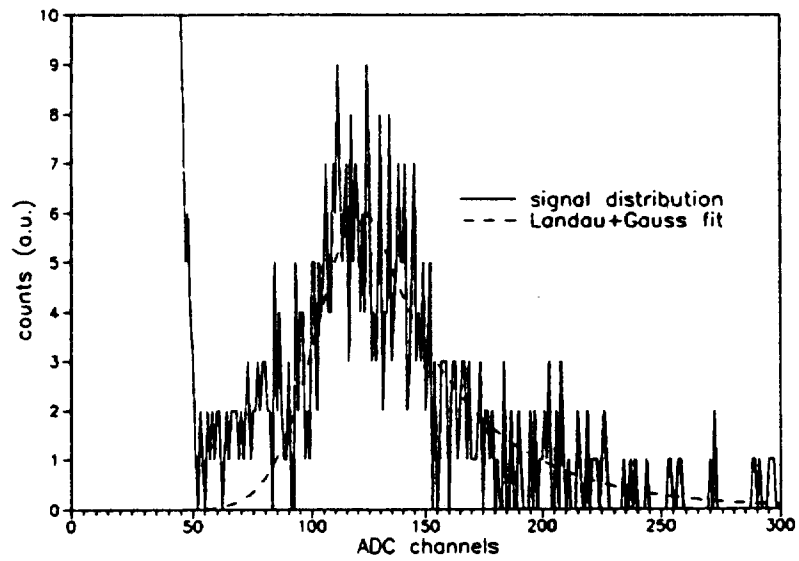


Figure 11: Spectrum of the signals for a single strip (pitch $50 \mu m$).